S & M 4191

# Dimethyl Sulfoxide–Enhanced Poly(3,4-ethylenedioxythiophene): Poly(styrenesulfonate) Hydrogels for Flexible and Conductive Sensors

Yen-Kai Huang, 1 Shih-Chen Shi, 1\* Guan-Yu Chen, 1 and Dieter Rahmadiawan 1,2

<sup>1</sup>Department of Mechanical Engineering, National Cheng Kung University (NCKU),
No. 1, University Road, Tainan 70101, Taiwan

<sup>2</sup>Department of Mechanical Engineering, Universitas Negeri Padang 25173 Padang, Sumatera Barat, Indonesia

(Received March 25, 2025; accepted September 25, 2025)

*Keywords:* conductive hydrogel, PEDOT:PSS modification, DMSO doping, wearable sensors, flexible electronics

Conductive hydrogels are promising materials for flexible and wearable sensors owing to their high conductivity, stretchability, and biocompatibility. However, the insulating nature of poly(styrene sulfonate) (PSS) in poly(3,4-ethylenedioxythiophene) (PEDOT) limits charge transport. Dimethyl sulfoxide (DMSO) has been used to enhance conductivity by modifying hydrogen bonding interactions. In this research, we incorporated DMSO into PEDOT:PSS hydrogels to improve conductivity. Fourier transform infrared spectroscopy confirmed that DMSO replaced hydrogen bonds between PEDOT and PSS, as shown by the disappearance of the SO<sub>3</sub><sup>-</sup> and S<sup>+</sup> peak at 1150 cm<sup>-1</sup> and the emergence of a –SO<sub>2</sub>H and O<sup>-</sup> peak at 1300 cm<sup>-1</sup>. Electrical measurements showed that resistance decreased from 200 to 40 kΩ, reaching 20% of its initial value. However, further DMSO addition led to conductivity saturation. These findings demonstrate that DMSO effectively enhances PEDOT:PSS hydrogels by improving charge transport. The enhanced conductivity makes these hydrogels suitable for wearable sensors, biomedical monitoring, and flexible electronics. Future research will focus on optimizing mechanical properties and stability for real-world applications.

### 1. Introduction

In recent years, the use of biodegradable materials has attracted significant attention owing to growing environmental concerns and the demand for sustainable alternatives in various applications.<sup>(1-6)</sup> In the realm of wearable electronics, where skin-compatible, lightweight, and environmentally friendly materials are critical, the integration of biodegradable polymers presents a promising solution.<sup>(7,8)</sup> Wearable devices, which are mobile electronic systems designed to adhere to human skin, have become essential for health monitoring, fitness tracking, and communication. As the demand for these devices increases, so does the need for flexible, durable, and environmentally friendly materials that can meet functional requirements without

<sup>\*</sup>Corresponding author: e-mail: <a href="mailto:scshi@mail.ncku.edu.tw">scshi@mail.ncku.edu.tw</a> <a href="mailto:https://doi.org/10.18494/SAM5641">https://doi.org/10.18494/SAM5641</a>

compromising sustainability. Wearable devices are mobile electronic systems that adhere to human skin, serving health monitoring, fitness tracking, and communication functions.

The global market for flexible electronics has been projected to grow from \$22 billion in 2022 to \$89.2 billion by 2030, with wearable sensors as one of the fastest-growing segments. In 2020, their market value was estimated at \$1.5 billion, with an annual growth rate of 10.7%. (9,10) Conductive hydrogels have emerged as key materials for wearable sensors owing to their stretchability, portability, and comfort. (11) Polyvinyl alcohol (PVA), a highly flexible and biocompatible polymer, is widely used in skin-contact hydrogels. (12–17)

Among conductive polymers, poly(3,4-ethylenedioxythiophene) (PEDOT):poly(styrene sulfonate) (PSS) has been recognized for its high conductivity, chemical stability, and ease of processing, making it widely applied in sensor hydrogels. (18) Moreover, PEDOT:PSS is widely recognized for its high electrical conductivity, mechanical flexibility, and biocompatibility, making it suitable for both implantable and skin-contact bioelectronic applications. (19) Despite PEDOT:PSS incorporation, hydrogel conductivity remains insufficient. (20)

In this study, we aim to enhance conductivity by introducing dimethyl sulfoxide (DMSO) to reduce PEDOT:PSS resistance. Previous studies have shown that PSS stabilizes PEDOT by preventing aggregation. However, its polystyrene backbone and sulfonic acid groups act as insulators, increasing resistance. Research has demonstrated that DMSO disrupts PEDOT:PSS hydrogen bonds, forming new interactions with sulfonic acid groups (-SO<sub>2</sub>H), which removes excess PSS and improves conductivity. In this study, we aim to optimize PEDOT:PSS-based hydrogels through controlled DMSO doping. Analyzing chemical interactions and conductivity changes contributes to developing high-performance, flexible conductive hydrogels for wearable sensors.

# 2. Materials and Methods

### 2.1 Preparation of PVA solution

PVA was dissolved in a glycerol-water mixture to prepare the solution. 3 g of PVA was added to 20 mL of deionized (DI) water and 20 mL of glycerol, followed by stirring at 80 °C and 300 RPM for 1.5 h to ensure complete mixing. The solution was then cooled to room temperature, forming a homogeneous PVA solution.

### 2.2 Preparation of conductive hydrogel

Acrylic acid (7 g), ammonium persulfate (0.5 g), tetramethylethylenediamine (0.01 mL), *N-N'*-methylene bisacrylamide (0.125 g), and cellulose nanocrystals (0.1 g) were mixed into the PVA solution. A specific amount of DMSO was combined with 10 mL of PEDOT:PSS via ultrasonication to achieve uniform dispersion before being added to the PVA/PAA aqueous solution. The mixture was stirred at 0 °C for 30 min to ensure thorough incorporation.

# 2.3 Formation of hydrogel network

The solution was placed in a 60 °C oven for 5 h to establish a covalently crosslinked PAA network. It was then frozen at -30 °C for 12 h, followed by thawing to room temperature, forming a secondary hydrogen-bonded crosslinked PVA network through freeze-thaw cycling.

# 2.4 Characterization of hydrogel

DMSO was used with Fourier transform infrared (FTIR) spectroscopy to verify the hydrogen bond substitution between PEDOT and PSS. A digital multimeter recorded the resistance changes in hydrogel patches containing various DMSO concentrations.

# 3. Results and Discussion

# 3.1 Effect of DMSO concentration on hydrogel appearance

The visual appearance of PVA/PAA conductive hydrogels with different DMSO concentrations was recorded, as shown in Fig. 1. As the DMSO concentration increased, notable differences were observed in the hydrogel samples. The samples with lower DMSO concentrations appeared more opaque, whereas those with higher concentrations exhibited increased transparency and improved uniformity.

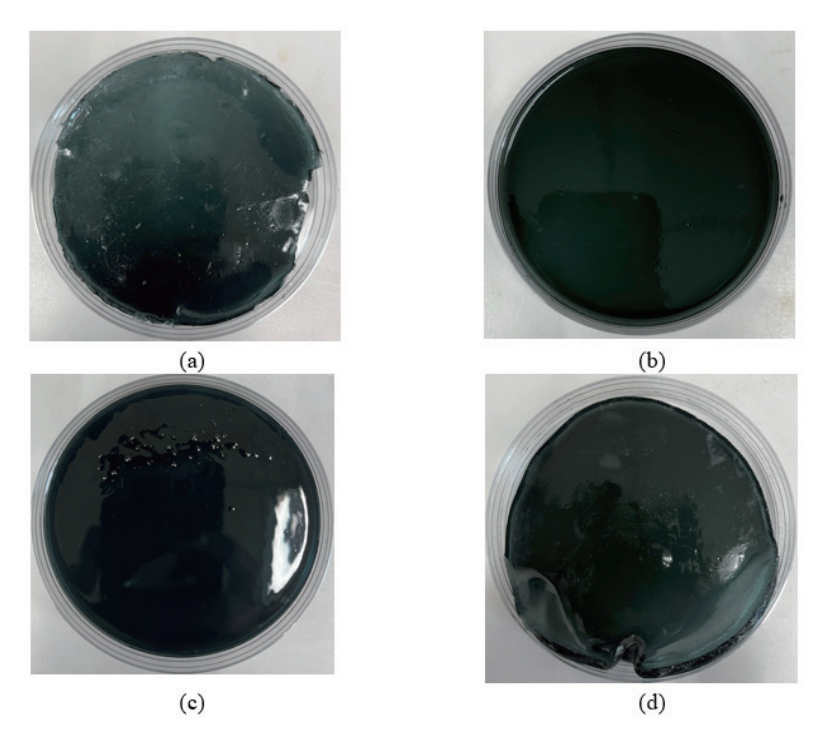


Fig. 1. (Color online) (a) DMSO 0% PVA/PAA conductive hydrogel, (b) DMSO 5% PVA/PAA conductive hydrogel, (c) DMSO 10% PVA/PAA conductive hydrogel, and (d) DMSO 15% PVA/PAA conductive hydrogel.

These changes indicate that DMSO affects the polymer network structure within the hydrogels. The increased transparency suggests improved phase compatibility between PEDOT:PSS and the PVA/PAA matrix, which can enhance charge transport pathways. Such morphological variations highlight the role of DMSO in modifying the structural and conductive properties of the hydrogels.

Thus, the appearance of the hydrogels demonstrates a correlation between DMSO concentration and the homogeneity of the conductive matrix. This observation aligns with previous studies that have reported the enhanced dispersion and compatibility of PEDOT:PSS in polymer matrices upon DMSO addition.

### 3.2 FTIR analysis of DMSO-induced bonding changes

FTIR spectroscopy was employed to quantitatively evaluate whether DMSO effectively replaced the original hydrogen bonding interactions between PEDOT and PSS (Fig. 2). The spectra revealed pronounced changes in the absorption region of 1050–1750 cm<sup>-1</sup>, corresponding to characteristic sulfonate and hydrogen-bonded structures in PEDOT:PSS.

In the pristine hydrogel (0 wt% DMSO), a distinct peak at 1150 cm<sup>-1</sup> was observed, assigned to the SO<sub>3</sub><sup>-</sup>···S<sup>+</sup> hydrogen bonds between the sulfonate groups of PSS and the PEDOT backbone. Upon DMSO incorporation, the intensity of this peak decreased progressively, with a total area reduction of ~45% at 15 wt% DMSO. Concurrently, a new absorption band appeared at ~1300 cm<sup>-1</sup>, attributed to -SO<sub>2</sub>H···O<sup>-</sup> hydrogen bonds formed between PSS and DMSO, showing an area increase of ~50% relative to the pristine sample.<sup>(25)</sup>

Peak position analysis revealed a slight redshift of the original 1150 cm<sup>-1</sup> band ( $\Delta v \approx -3$  cm<sup>-1</sup>) before its disappearance, indicating a weakening of the original PEDOT-PSS hydrogen bonding. The emergence of the 1300 cm<sup>-1</sup> band without significant broadening (*FWHM*  $\approx$  constant) suggests that DMSO selectively interacts with sulfonic acid groups rather than causing nonspecific polymer backbone distortion. These quantitative spectral shifts and intensity changes confirm that DMSO disrupts the insulating PSS matrix, reducing its content in the conductive network.<sup>(26)</sup>

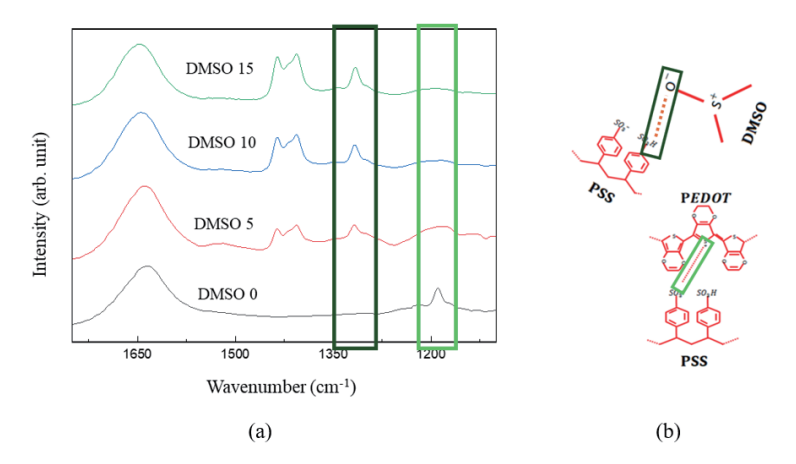


Fig. 2. (Color online) (a) FTIR spectra of hydrogels with various DMSO concentrations. (b) Hydrogen bonding structure between DMSO and PEDOT:PSS.

### 3.3 Bonding structure changes in conductive hydrogels

Figure 3 shows the bonding strength variations of PVA/PAA hydrogels with different DMSO concentrations. The characteristic peak disappearance at 1150 cm<sup>-1</sup> and the new peak at 1300 cm<sup>-1</sup> confirmed that DMSO successfully modified the bonding structure in PEDOT:PSS. These changes indicate that DMSO facilitated the breakdown of existing PEDOT-PSS hydrogen bonds and promoted new bonding interactions with PSS.

The ability of DMSO to alter hydrogen bonding interactions suggests that it plays a critical role in tuning the conductive properties of PEDOT:PSS-based hydrogels. DMSO enhanced electron transport pathways by reducing the presence of excess PSS, which previously acted as an insulating barrier. This improvement is critical for applications requiring efficient charge conduction, such as wearable sensors.

Thus, the bonding structure modifications induced by DMSO demonstrate its effectiveness in optimizing the electrical properties of conductive hydrogels. These findings align with previous reports highlighting the role of DMSO as a secondary dopant in improving PEDOT:PSS conductivity.

# 3.4 Conductivity enhancement by DMSO addition

Figures 3(a) and 3(b) demonstrate the significant impact of DMSO on the electrical conductivity of the hydrogels. The resistance decreased considerably from approximately 200 k $\Omega$  in the absence of DMSO to around 40 k $\Omega$  when the DMSO concentration reached 15%. Beyond this concentration, the reduction in resistance stabilized, indicating a saturation effect in conductivity improvement.

The observed reduction in resistance confirms that DMSO effectively replaced insulating PSS components, thereby increasing charge carrier mobility within the hydrogels. This enhancement is attributed to removing excess PSS, which previously acted as an electron-blocking layer. As a result, the PEDOT:PSS network became more interconnected, facilitating more efficient charge transport.

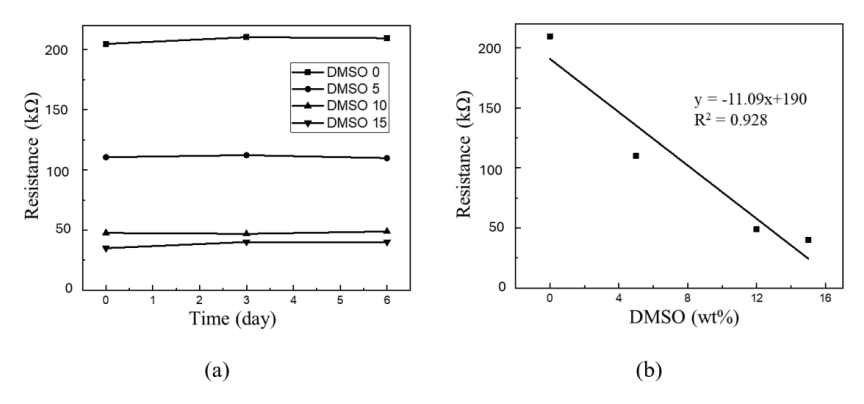


Fig. 3. (a) Conductivity retention in hydrogels with various DMSO concentrations. (b) Conductivity measurements of hydrogels with different DMSO concentrations.

For comparison, pure PEDOT:PSS hydrogels enhanced with additives such as ionic liquids, glycerol, or DMSO achieve conductivities around 40 S/cm, whereas stretchable PEDOT:PSS hydrogels exhibit even higher values, up to 74 S/cm for certain formulations. In a template-directed design (T-ECH), a record-high conductivity of 247 S/cm has been demonstrated. Despite not reaching these extremely high conductivity levels, our hydrogels achieve a substantial fivefold resistance reduction (from ~200 to ~40 k $\Omega$ ) while maintaining favorable flexibility and stability, making them competitive for practical wearable sensor applications. The conductivity adjustment achieved through DMSO incorporation demonstrates its potential for optimizing wearable sensor materials, and the ability to tune conductivity by varying DMSO concentration suggests that this method can be applied in designing flexible and efficient bioelectronic devices.

# 3.5 Stability of conductive hydrogels

Resistance measurements were performed over six days to evaluate the conductive hydrogels' stability. As shown in Fig. 3, the resistance values remained unchanged throughout this period, indicating that the hydrogels maintained their conductivity over time. This stability is essential for practical applications, particularly in wearable electronics, where long-term reliability is required.

The stability of the hydrogels suggests that the conductive network formed by PEDOT:PSS remained intact despite prolonged exposure to environmental conditions. This observation aligns with previous findings that have reported high durability in PEDOT:PSS-based materials when adequately doped, and the six-day evaluation period is in line with similar short-term stability tests reported in the literature.<sup>(29)</sup>

Note that the base hydrogel network employed here has been mechanically characterized in our previous work, (30) exhibiting a tensile strength of up to ~450 kPa and an elongation at break of up to ~980%. Such high stretchability and strength not only ensure mechanical durability under repeated deformation but also contribute to long-term structural stability, which is essential for skin-conformal wearable electronics. These properties are expected to remain comparable in the present system, as the fabrication process is identical apart from the DMSO adjustment.

## 3.6 Verification of conductivity using a simple circuit

A simple light bulb circuit was constructed to validate the conductivity improvements further, incorporating hydrogels with various DMSO concentrations. As illustrated in Fig. 4, the light bulb's brightness increased progressively as the DMSO concentration increased from 0 to 15%. This trend confirms that higher DMSO concentrations lead to lower resistance and improved charge conduction.

The gradual increase in brightness demonstrates the direct impact of DMSO on the electrical properties of the hydrogels. The improved conductivity allowed more current to flow through the circuit, resulting in higher light intensity. These results further reinforce the hypothesis that DMSO effectively enhances the charge transport capability of PEDOT:PSS-based hydrogels.

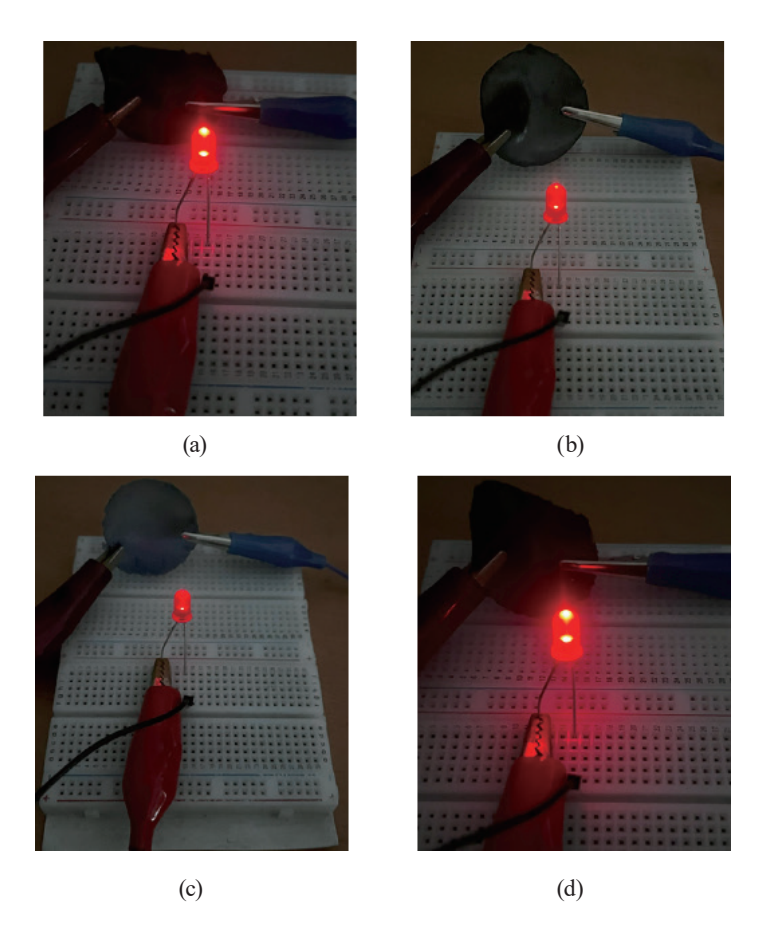


Fig. 4. (Color online) Simple light bulb circuit with (a) DMSO 0 wt% conductive hydrogel, (b) DMSO 5 wt% conductive hydrogel, (c) DMSO 10 wt% conductive hydrogel, and (d) DMSO 15 wt% conductive hydrogel.



Fig. 5. (Color online) Schematic illustration of the role of DMSO in enhancing the electrical conductivity of the PVA/PAA conductive hydrogel. DMSO interacts with PEDOT:PSS chains, improving charge transport and resulting in higher conductivity for the hydrogel.

Therefore, the visual confirmation of increased conductivity supports the findings obtained from FTIR and resistance measurements.

The ability of DMSO to significantly enhance electrical performance suggests that it can be a viable strategy for improving wearable sensor materials. Figure 5 shows how DMSO enhances the electrical conductivity of the PVA/PAA conductive hydrogel. By interacting with PEDOT:PSS chains, DMSO improves charge transport pathways, leading to a more efficient current flow through the hydrogel.

### 4. Conclusion

In this study, we demonstrated that adding DMSO enhanced the conductivity of PEDOT:PSSbased hydrogels by effectively replacing hydrogen bonding between PEDOT and PSS. FTIR analysis showed that the SO<sub>3</sub><sup>-</sup> and S<sup>+</sup> hydrogen bonding peak at 1150 cm<sup>-1</sup> disappeared, whereas a new -SO<sub>2</sub>H and O<sup>-</sup> peak at 1300 cm<sup>-1</sup> emerged, confirming the successful replacement of insulating components. Electrical resistance measurements revealed a significant reduction, from approximately 200 to around 40 k $\Omega$ , reaching 20% of its initial value. However, further DMSO addition led to a plateau in conductivity improvement, suggesting a saturation limit. These findings confirm the role of DMSO in enhancing conductivity and optimizing PEDOT:PSS-based hydrogels for sensor applications. The improved conductivity enhances signal quality, energy efficiency, and stability, which makes these materials highly suitable for wearable and flexible sensors. Their stable and precise electrical response in biomedical monitoring supports accurate physiological signal detection. Beyond biomedical applications, these conductive hydrogels exhibit promise for flexible electronics, energy storage, and humanmachine interfaces. Their high conductivity and mechanical flexibility position them as viable candidates for next-generation electronic devices. The ability to systematically tune resistance through DMSO incorporation demonstrates their adaptability for various advanced sensor applications. Future research will explore long-term stability, biocompatibility, and durability for real-world applications. Optimizing hydrogel formulations will enhance sensor performance and integration into flexible electronic systems. These advancements will contribute to developing energy-efficient, high-performance wearable sensors supporting innovations in bio-integrated electronics.

In this study, we demonstrated the feasibility of DMSO-assisted conductivity enhancement in PEDOT:PSS-based hydrogels. These materials offer a promising platform for next-generation conductive hydrogel sensors, advancing wearable electronics and flexible device technology.

# Acknowledgments

This work was supported by the National Science and Technology Council, Taiwan (grant numbers 112-2221-E-006-173, 113-2221-E-006-087-MY2, 113-2221-E-006-112-MY2, 113-2221-E-006-116, and 114-2221-E-006-090). We are grateful to the Core Facility Center of National Cheng Kung University for providing access to the EM000700 equipment. We are also grateful for the partial support of the Higher Education Sprout Project, Ministry of Education through the Headquarters of University Advancement at National Cheng Kung University (NCKU).

### References

- 1 N. Sandra, M. A. Caronge, J. Sunaryati, K. Kawaai, W. Nsama, Y. Arbi, and A. S. R. Arifin: Teknomekanik 8 (2025) 79. https://doi.org/10.24036/teknomekanik.v8i1.34572
- A. N. Fauza, F. Qalbina, H. Nurdin, A. Ambiyar, and R. Refdinal: Teknomekanik 6 (2023) 21. <a href="https://doi.org/10.24036/teknomekanik.v6i1.21472">https://doi.org/10.24036/teknomekanik.v6i1.21472</a>
- 3 H. Nurdin, W. Waskito, A. N. Fauza, B. M. Siregar, and B. K. Kenzhaliyev: Teknomekanik 6 (2023) 94. <a href="https://doi.org/10.24036/teknomekanik.v6i2.25972">https://doi.org/10.24036/teknomekanik.v6i2.25972</a>

- 4 A. Amri, D. E. Putri, D. Febryza, S. D. Voadi, S. P. Utami, H. A. Miran, and M. M. Rahman: Teknomekanik 7 (2024) 139. https://doi.org/10.24036/teknomekanik.v7i2.32972
- 5 D. Rahmadiawan, H. Abral, M. A. Azka, S. M. Sapuan, R. I. Admi, S. C. Shi, R. Zainul, Azril, A. Zikri, and M. Mahardika: RSC Adv. 14 (2024) 29624. https://doi.org/10.1039/d4ra06099g
- 6 S.-C. Shi, F.-I. Lu, C.-Y. Wang, Y.-T. Chen, K.-W. Tee, R.-C. Lin, H.-L. Tsai, and D. Rahmadiawan: Int. J. Biol. Macromol. 264 (2024) 130547. https://doi.org/10.1016/j.ijbiomac.2024.130547
- 7 Z. Zhai, X. Du, Y. Long, and H. Zheng: Front. Electron. 3 (2022). https://doi.org/10.3389/felec.2022.985681
- 8 C. Sharma, Y. S. Negi, and K. Parida: Biodegradable Polymers for Wearable Electronics and Device Fabrication, Encyclopedia of Green Materials (Springer Nature Singapore, Singapore, 2022) p. 1. <a href="https://doi.org/10.1007/978-981-16-4921-9">https://doi.org/10.1007/978-981-16-4921-9</a> 195-1
- 9 S. N. Banitaba, S. Khademolqorani, V. V. Jadhav, E. Chamanehpour, Y. K. Mishra, E. Mostafavi, and A. Kaushik: Mater. Today Electron. 5 (2023). <a href="https://doi.org/10.1016/j.mtelec.2023.100055">https://doi.org/10.1016/j.mtelec.2023.100055</a>
- D. Corzo, G. Tostado-Blázquez, and D. Baran: Front. Electron. 1 (2020). <a href="https://doi.org/10.3389/felec.2020.594003">https://doi.org/10.3389/felec.2020.594003</a>
- Y. Liu, L. Wang, Y. Mi, S. Zhao, S. Qi, M. Sun, B. Peng, Q. Xu, Y. Niu, and Y. Zhou: J. Mater. Chem. C 10 (2022) 13351. <a href="https://doi.org/10.1039/d2tc01104b">https://doi.org/10.1039/d2tc01104b</a>
- 12 H. Ding, J. Liu, X. Shen, and H. Li: Polymers 15 (2023) 4001. https://doi.org/10.3390/polym15194001
- 13 D. Rahmadiawan, H. Abral, I. Chayri Iby, H. J. Kim, K. H. Ryu, H. W. Kwack, M. Razan Railis, E. Sugiarti, A. Novi Muslimin, D. Handayani, K. Dwinatrana, S. C. Shi, R. Zainul, and R. Azis Nabawi: Heliyon 10 (2024) e30748. https://doi.org/10.1016/j.heliyon.2024.e30748
- 14 D. Rahmadiawan, S.-C. Shi, and W.-T. Zhuang: Mater. Res. Express 11 (2024) 115302. <a href="https://doi.org/10.1088/2053-1591/ad8f94">https://doi.org/10.1088/2053-1591/ad8f94</a>
- 15 C.-T. Chou, S.-C. Shi, and C.-K. Chen: Polymers 13 (2021) 4447. https://doi.org/10.3390/polym13244447
- 16 S.-C. Shi, T.-H. Chen, and P. K. Mandal: Polymers 12 (2020) 1246. https://doi.org/10.3390/polym12061246
- 17 D. Rahmadiawan, H. Abral, M. A. Pratama, H.-J. Kim, R. M. Railis, R. Kurniawan, S. R. Putri Primandari, S.-C. Shi, and M. Mahardika: RSC Adv. 15 (2025) 2766. https://doi.org/10.1039/D4RA08801H
- 18 G. Li, C. Li, G. Li, D. Yu, Z. Song, H. Wang, X. Liu, H. Liu, and W. Liu: Small 18 (2022) 2101518. <a href="https://doi.org/10.1002/sml1.202101518">https://doi.org/10.1002/sml1.202101518</a>
- 19 J. Li, D. Mo, J. Hu, S. Wang, J. Gong, Y. Huang, Z. Li, Z. Yuan, and M. Xu: Microsyst. Nanoeng. **11** (2025) 87. : <a href="https://doi.org/10.1038/s41378-025-00948-w">https://doi.org/10.1038/s41378-025-00948-w</a>
- C. Zhou, T. Wu, X. Xie, G. Song, X. Ma, Q. Mu, Z. Huang, X. Liu, C. Sun, and W. Xu: Eur. Polym. J. 177 (2022) 111454. <a href="https://doi.org/10.1016/j.eurpolymj.2022.111454">https://doi.org/10.1016/j.eurpolymj.2022.111454</a>
- 21 X. Fan, N. E. Stott, J. Zeng, Y. Li, J. Ouyang, L. Chu, and W. Song: J. Mater. Chem. A **11** (2023) 18561. <a href="https://doi.org/10.1039/D3TA03213B">https://doi.org/10.1039/D3TA03213B</a>
- 22 Y. H. Kim, C. Sachse, M. L. Machala, C. May, L. Müller-Meskamp, and K. Leo: Adv. Funct. Mater. **21** (2011) 1076. <a href="https://dx.doi.org/10.1002/adfm.201002290">https://dx.doi.org/10.1002/adfm.201002290</a>
- 23 I. Cruz-Cruz, M. Reyes-Reyes, M. Aguilar-Frutis, A. Rodriguez, and R. López-Sandoval: Synth. Met. 160 (2010) 1501. https://doi.org/j.synthmet.2010.05.010
- 24 I. Lee, G. W. Kim, M. Yang, and T.-S. Kim: ACS Appl. Mater. Interfaces 8 (2016) 302. <a href="https://doi.org/10.1021/acsami.5b08753"><u>https://doi.org/10.1021/acsami.5b08753</u></a>
- H. Yousefian, A. Babaei-Ghazvini, A. A. Isari, S. A. Hashemi, B. Acharya, A. Ghaffarkhah, and M. Arjmand: Surf. Interfaces **51** (2024) 104481. <a href="https://doi.org/https://doi.org/10.1016/j.surfin.2024.104481">https://doi.org/https://doi.org/10.1016/j.surfin.2024.104481</a>
- 26 P. Sakunpongpitiporn, K. Phasuksom, N. Paradee, and A. Sirivat: RSC Adv. 9 (2019) 6363. <a href="https://doi.org/10.1039/C8RA08801B">https://doi.org/10.1039/C8RA08801B</a>
- 27 M. S. Rahman, A. Shon, R. Joseph, A. Pavlov, A. Stefanov, M. Namkoong, H. Guo, D. Bui, R. Master, A. Sharma, J. Lee, M. Rivas, A. Elati, Y. Jones-Hall, F. Zhao, H. Park, M. A. Hook, and L. Tian: Sci. Adv. 11 (2025) eads4415. <a href="https://doi.org/10.1126/sciadv.ads4415">https://doi.org/10.1126/sciadv.ads4415</a>
- 28 J. Chong, C. Sung, K. S. Nam, T. Kang, H. Kim, H. Lee, H. Park, S. Park, and J. Kang: Nat. Commun. **14** (2023) 2206. https://doi.org/10.1038/s41467-023-37948-1
- 29 H. Xue, D. Wang, M. Jin, H. Gao, X. Wang, L. Xia, D. Li, K. Sun, H. Wang, X. Dong, C. Zhang, F. Cong, and J. Lin: Microsyst. Nanoeng. 9 (2023) 79. <a href="https://doi.org/10.1038/s41378-023-00524-0">https://doi.org/10.1038/s41378-023-00524-0</a>
- 30 S.-C. Shi, S.-T. Cheng, and D. Rahmadiawan: Sens. Actuators, A **379** (2024) 115981. <a href="https://doi.org/https://doi.org/10.1016/j.sna.2024.115981">https://doi.org/https://doi.org/10.1016/j.sna.2024.115981</a>